Compression waves reflection from the low-velocity azimuthally anisotropic medium: A physical model study

Yu.I. Kolesnikov[1,2], K.V. Fedin[1,3,4], L. Ngomayezwe[3]

[1]Trofimuk Institute of Petroleum Geology and Geophysics SB RAS, Akademika Koptyuga Pr. 3, 630090 Novosibirsk, Russia, [2]Seismological Branch of Unified Geophysical Service RAS, Akademika Koptyuga Pr. 3, 630090 Novosibirsk, Russia, [3]Novosibirsk State University, Pirogova Street 2, 630090 Novosibirsk, Russia, and [4]Novosibirsk State Technical University, Department of Geophysical Systems, 630073, Novosibirsk, Karl Marx Prosp., 2, Russia.

Fax +7(383)330-28-07, e-mail : kolesnikovyi@ipgg.sbras.ru, fedinkv@ipgg.sbras.ru, Lngomayezwe@gmail.com

Corresponding author **:** *kolesnikovyi@ipgg.sbras.ru*

Interest in azimuthal anisotropy of rocks is mainly associated with fractured reservoirs, which may contain hydrocarbon deposits. Cracks in such deposits in most cases have a subvertical orientation, which is caused by the predominance of vertical stresses in rocks over horizontal ones. To determine the azimuthal direction of fractures, one can use, in particular, the dependence of the reflection coefficients of elastic waves on the boundaries with such media on the azimuth. This paper presents the results of physical modelling, demonstrating this dependence. To conduct experiments, we developed a technology for manufacturing models of azimuthally anisotropic (HTI) media with a high degree of anisotropy by 3D printing. The features of the reflection of compression waves from the boundary of water and low-velocity azimuthally anisotropic media were experimentally investigated on the example of the model HTI medium produced by this method. Experiments have shown that at angles of incidence less than 25°, the reflection coefficients are practically independent from the azimuth. However, at larger angles of incidence, an azimuthal dependence of the reflection coefficients

is observed, most pronounced at azimuths from 45° to 75°. The results of measurements in the direction of the isotropy plane agree well with the theoretical reflection coefficients for the boundary of isotropic media.

Keywords: *Azimuthally anisotropic medium, compression waves, reflection coefficients, physical modelling*

INTRODUCTION

Seismic anisotropy, that is, the dependence of the elastic properties of the medium on the direction of wave propagation, can be caused by various reasons, which are: the orderly arrangement of grains of rock-forming minerals, the thin-layer structure of rocks, their fracturing, etc. In anisotropic media, both the velocities and the attenuation of seismic waves may depend on the direction. There are also well-known effects associated with seismic anisotropy such as the splitting of shear waves into fast and slow, the triplication of *SV*-wave fronts in some cases, the dependence of the reflection and transmission coefficients on the anisotropic properties of bordering media (Tsvankin 2012).

In recent years, an increased interest in manifestations of rock anisotropy has been associated with fractured reservoirs, which may contain hydrocarbon deposits (Helbig & Thomsen 2005; Liu *et al.* 2007; Worthington 2008; Cao *et al.* 2018). Cracks in such deposits in most cases have a subvertical orientation, which is caused by the predominance of vertical stresses in rocks over horizontal ones. The azimuthal direction of such fracturing is an important characteristic of fractured reservoirs, as it should be considered at different stages of design development and operation of oil and gas fields.

In the first approximation, rocks with vertical fracturing can be considered as a transversely isotropic medium with a horizontal axis of symmetry (HTI model), or an

azimuthally anisotropic medium. Therefore, in practice, the dependence of the reflection coefficients on the azimuth can be used to determine the direction of preferential orientation of cracks in reservoirs, for example, using AVO-analysis methods developed for azimuthally anisotropic media (Lynn *et al*. 1996; Mallick *et al*. 1998; Jenner 2002; Hall & Kendall 2003). For testing and reliable verification of such methods, simulation data, including data of physical modelling, should be used.

For the physical modelling of anisotropic media, one can use ready-made materials, which have anisotropic properties, such as cloth-based or paper-based laminates (Broun *et al*. 1991; Cheadle *et al*. 1991; Chang *et al*. 1994, 1995; Chang & Gardner 1997; Chang & Chang 2001; Mah & Schmitt 2001). The packs of thin plates of glass, aluminum or other sheet materials, glued together, for example, by epoxy resin, can also be used as anisotropic materials (Melia & Carlson 1984; Ebrom *et al*. 1990b). Industrial layered materials are sufficiently homogeneous, but usually characterized by a relatively low degree of anisotropy. In the artisanal manufacture of thin-layered materials, it is difficult to ensure their uniformity, in particular, to maintain a constant thickness of the layers of the bonding material.

Another method of obtaining a solid anisotropic material for laboratory experiments is described in the paper (Luan *et al*. 2016). The authors mixed powders of various minerals with their subsequent pressing, after which the artificial samples had a layered microstructure like natural shale. The manufacturing techniques of such samples are quite laborious, and it is not obvious whether they are obtained sufficiently homogeneous after pressing.

Fractured media are modeled, as a rule, by packs of thin plates, for example, from plexiglass, sometimes with thin layers of water subjected to compression along the axis of symmetry (Ebrom *et al*. 1990a; Tatham *et al*. 1992). For the manufacture of more complex

models of fractured media with controlled fracture geometry, a similar technology is proposed, but with the inclusion of thin foil films with cutouts simulating cracks between the plexiglass plates (Karaev *et al*. 2008). The disadvantages of such models include some technical problems that may arise during the experiments, which is associated with the need to ensure uniform compression of the plates.

Finally, 3D printing technologies that have been developing in recent years have made it possible to create thin-layered models with well-controlled properties. Such models are used, for example, in medicine for teaching ultrasound diagnostic methods (Robertson et al. 2016). Ultrasound, on the other hand, is used to test various objects printed on a 3D printer (Zeltmann et al. 2016). Apparently, the first experience of creating such models of rocks is described in the paper (Huang *et al*. 2016). We used just 3D printing technology to model azimuthally anisotropic medium.

In the previously published works on physical modelling of compression wave reflection from the boundaries with azimuthally anisotropic media, the paper-based laminate (Chang & Gardner 1997) or the cloth-based laminate (Mahmoudian *et al*. 2015; Malehmir & Schmitt 2017) were used. The velocities of the compression waves in these materials are higher than in the media, in which the incident and reflected waves propagated. This paper presents the results of a physical modelling of the reflection of compression waves from the boundary of water with a low-velocity azimuthally anisotropic medium, that is, for the case when there are no critical angles.

MODEL OF AN AZIMUTHALLY ANISOTROPIC MEDIUM

Considering the peculiarities of the experimental technique we used, relatively small ($10\times10\times3$ cm^3) sizes of the material sample modelling the azimuthally anisotropic medium were chosen. We have developed and used the following technology to manufacture a model of HTI medium with a high degree of anisotropy. The sample of transversely isotropic material used in this study was printed on a 3D-printer Raise3D N2 Dual by the method of layer-by-layer fusing of acrylonitrile butadiene styrene (ABS plastic) 0.1 mm thick threads. Vertical layering was simulated by alternating 0.2 mm thick layers with different densities and elastic properties. The structure of the sample is schematically shown in Fig. 1a.

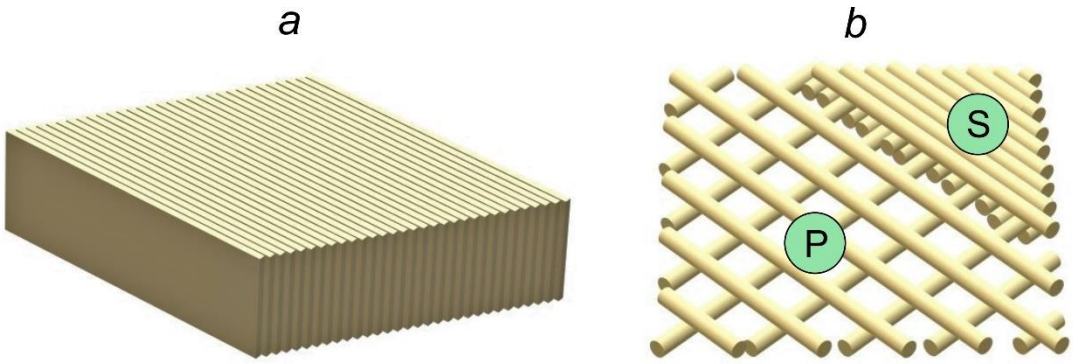

Figure. 1. (a) The structure of an azimuthally anisotropic material printed on a 3D printer; (b) an arrangement of ABS plastic threads in double "solid" (S) and "porous" (P) sample layers.

The process of making a sample began with printing one of its side faces with size 10×3 cm^3. First, a layer of plastic threads was printed, laid without gaps parallel to each other in a single row at an angle of 45 degrees to the edges of the sample. The same layer was placed on top of this layer with threads laid perpendicular to the threads of the underlying layer. Thus, the first "solid" double layer of 0.2 mm thickness was formed.

Then, a "porous" double layer, also 0.2 mm thick, was printed on top of this "solid" double layer. The structure of this layer was similar to the structure of the "solid" layer, but gaps were left between its adjacent threads. The relative position of the plastic threads in the "solid" and "porous" double layers is shown in Fig. 1b. Further printing alternated these "solid" and "porous" double layers until the complete formation of a sample with size $10\times10\times3$ cm^3.

The density of a "solid" material measured from the specially printed reference sample without porous layers was ρ_s =0.92 g/cm^3. Considering the certified value of density of ABS plastic (ρ_{ABS} =1.04 g/cm^3), the porosity of these layers is equal to $(1-\rho_s/\rho_{ABS})$, that is approximately 11.5%. To obtain a sample with relatively large values of the anisotropy coefficients, the printing of the "porous" double layers was programmed with a ten percent filling with threads. The measured density of the entirely finished layered sample was ρ =0.52 g/cm^3, therefore, its total porosity determined by the formula $(1-\rho/\rho_{ABS})$, is approximately 50%. All layers in the sample had the same thickness of 0.2 mm, which implies that the porosity of the "porous" double layers is close to 88.5%, and their density is ρ_p =0.12 g/cm^3.

Such a combined layered sample can be considered a rock model with cracks partially filled with solid material. The watertightness of the sample was provided by a "solid" layer of plastic 0.1 mm thick printed on the surface of all faces. To control the watertightness, the sample was weighed on an electronic laboratory balance (accuracy 0.01 g) and then kept in water for approximately 24 hours. After that, a control weighing of the sample was carried out, which showed no noticeable change in its mass.

Measuring the velocity of compression waves in two main directions gave the values of V_{p1} =1110 m/s for the fast wave (along the layering) and V_{p2} =795 m/s for the slow wave (across the layering). For shear waves, the following velocities of fast and slow waves were obtained: V_{s1} =680 m/s and V_{s2} =485 m/s. In terms of stiffness coefficients c_{ij} and sample density ρ these velocities can be defined as $V_{p1} = \sqrt{c_{11}/\rho}$, $V_{p2} = \sqrt{c_{33}/\rho}$, $V_{s1} = \sqrt{c_{66}/\rho}$, $V_{s2} = \sqrt{c_{55}/\rho}$ (Tsvankin 2012). Thus, for this sample, the anisotropy coefficients for both compression and shear waves defined as $æ_p = V_{p1}/V_{p2}$ and $æ_s = V_{s1}/V_{s2}$ turned out to be equal approximately to 1.4. The measured velocity of compression waves in water was 1502 m/s, the density of water was 1 g/cm^3.

EXPERIMENTAL TECHNIQUE

The methodology of the experiments practically did not differ from the previously one used to determine the reflection coefficients from the boundary of water with non-ideally elastic media (Kolesnikov 2005). The schematic diagram of the experiments is shown in Fig. 2a. To vary the angles of incidence α, a lever device was used (Fig. 2b). The change of azimuth β of the plane of incidence relative to the plane of isotropy was made by rotating the sample around the vertical axis. Fig. 3c shows how the angle of incidence and the azimuth of the plane of incidence are determined.

The lever device allowed rotating the source and receiver (hereinafter referred to as sensors) of ultrasonic pulses on independent levers of fixed length around an imaginary axis passing along the flat upper boundary of the test sample. In this case, the axes of maximum sensitivity of the sensors were always oriented perpendicular to the axis of rotation of the levers.

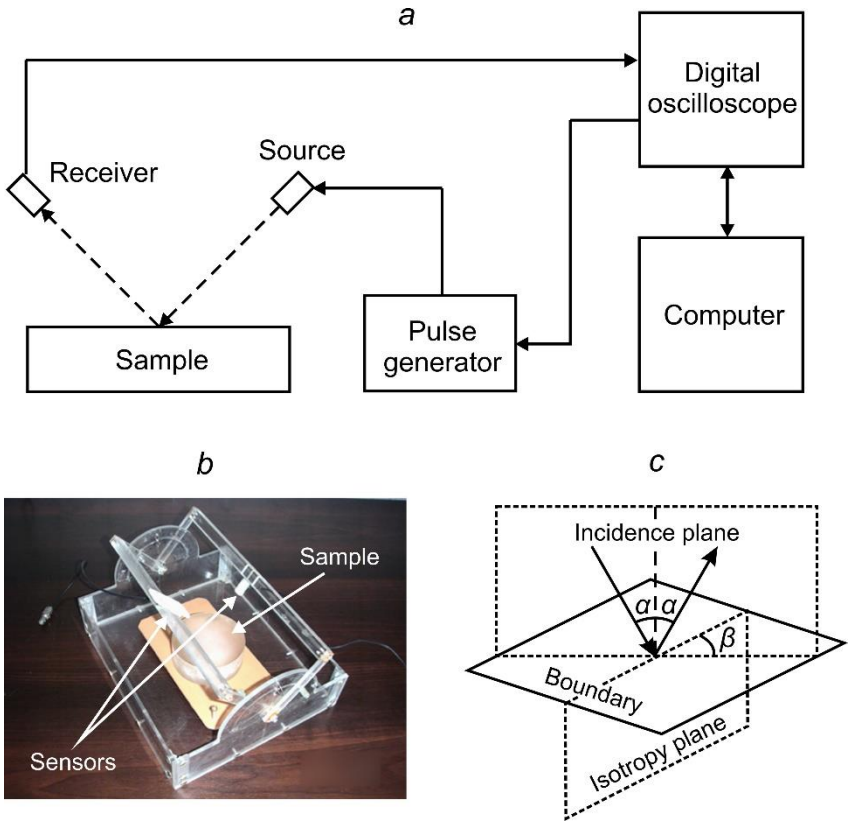

Figure 2. (a) The schematic diagram of the experiment, (b) the design of the lever device and (c) the definition of incidence angle α and azimuth β.

For each measurement, the levers with sensors were set at the same angles to the sample surface. In the course of obtaining experimental data on the dependence of the reflection coefficients on the angle of incidence, these angles changed synchronously in opposite directions with a step of 5°. Thus, at any angle of inclination of the levers, the center of the reflecting segment was in the same place. This technique allowed us to minimize the influence of sensor directional diagrams on the measurement results.

Piston-type sensors were made from piezoceramic disks with a thickness of 1 mm and a diameter of 6 mm (source) and 10 mm (receiver). The distance from the axis of rotation to the source was 64 mm, to the receiver – 70 mm. The length of the ray path incident on the

border and then reflected from it was thus 134 mm. For shielding of the direct wave arriving in the first arrivals, a thin foam plastic plate was placed between the sensors. The whole construction together with the sample was placed in a container with water at the time of the experiment.

For excitation of compression waves in water, rectangular electrical pulses with duration of 1 microsecond and amplitude of 60 volts were applied to the source. The ultrasonic pulses reflected from the water-sample boundary were converted by the receiver into electrical signals, which after amplification were recorded by the B-423 digital oscilloscope on the computer hard disk for further processing.

The sampling rate of analog signals during digitization was 200 MHz. To increase the signal-to-noise ratio, a 1000-fold accumulation of signals was made. An example of an experimental seismogram for an azimuth of 45° is shown in Fig. 3. It can be seen from the figure that the recorded pulses have the form of a damped sinusoid with a predominant frequency of about 1.8 MHz. The wavelength in water at this frequency is 0.83 mm, which is about an order of magnitude greater than the thickness of the plastic threads from which the model was printed.

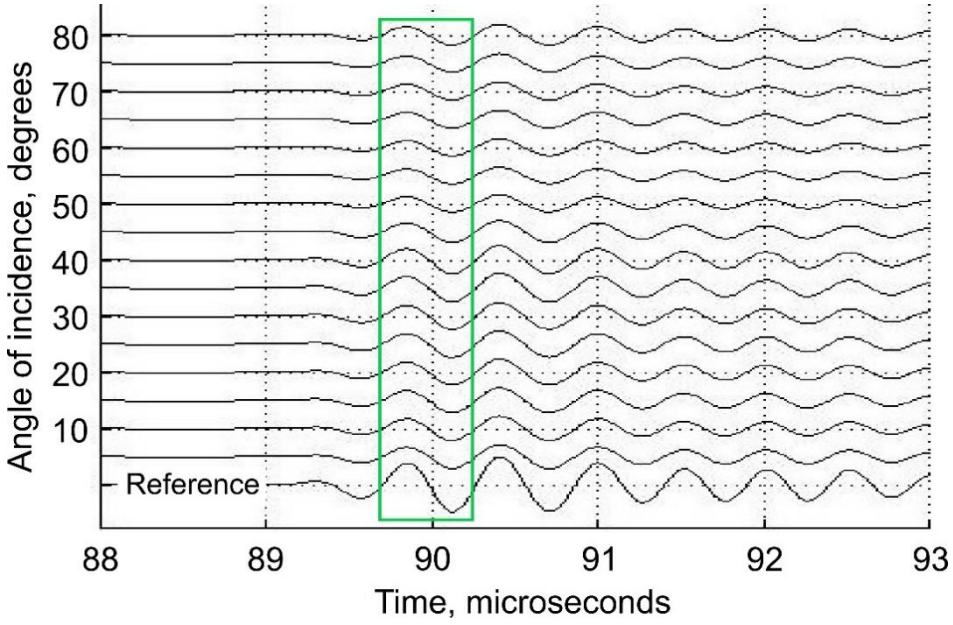

Figure 3. Example of experimental ultrasonic seismogram for azimuth of 45°.

When processing the experimental data for each angle of incidence, the amplitude of the reflected signal (difference of maximum and minimum) was measured in the time window highlighted in Fig. 3 rectangular outline. To calculate the reflection coefficient modules, the amplitude of each signal was divided by the amplitude of the "reference" direct wave (bottom trace in Fig. 3):

$$|R| = \frac{A^r_{max} - A^r_{min}}{A^d_{max} - A^d_{min}},$$

where A^r_{max} and A^r_{min} – the maximum and minimum amplitudes of the reflected wave, A^d_{max} and A^d_{min} – the maximum and minimum amplitudes of the "reference" direct wave measured in the same time window shown in rectangular outline, Fig. 3.

The "reference" wave was recorded in water in the absence of a sample with a coaxial arrangement of sensors at a distance of 134 mm, equal to the length of the ray path when

recording reflected waves. Thus, the influence of the geometrical spreading on the measurement results was compensated.

RESULTS AND DISCUSSION

During the experiments, the dependences of the modulus of the reflection coefficient on the angles of incidence (in the range from 5° to 80°) were obtained with a step of 5°. These dependences were determined for the azimuthal directions of the plane of incidence from 0° (along layering) to 90° (across layering) also with a step of 5°. The graphs of the reflection coefficient module dependence on the angle of incidence for some azimuths are shown in Fig. 4.

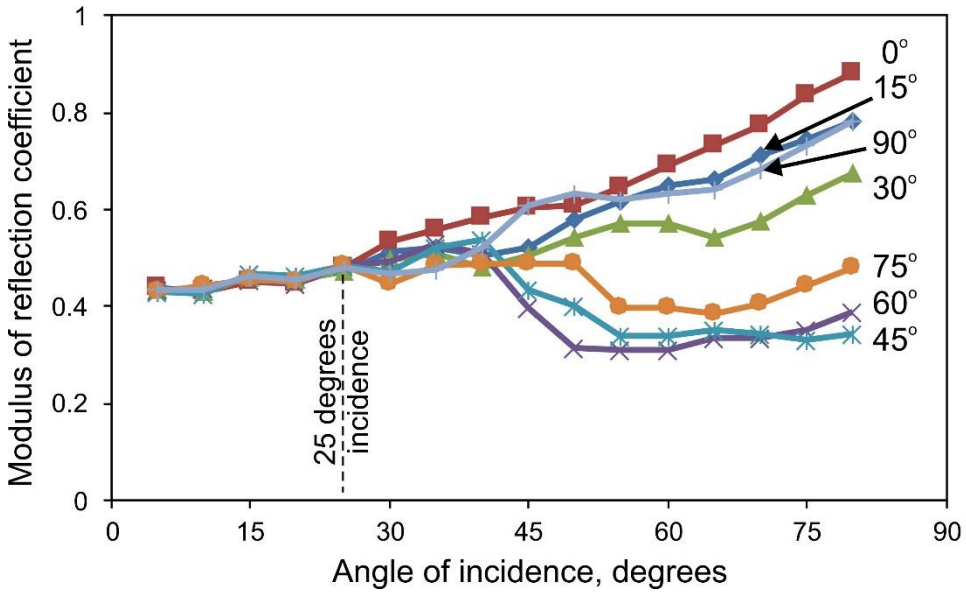

Figure 4. The dependence of the reflection coefficient on the angle of incidence on the boundary of water with an azimuthally anisotropic sample for some azimuths of the plane of incidence relative to the direction of layering (0° – along, 90° – across the layering).

It can be seen that, for angles of incidence less than 25°, the reflection coefficient modules for different azimuths are practically the same. However, for large angles there is an azimuthal dependence of this parameter. It has maximum values at azimuths close to 0° and

90° (these are the directions along and across the layering). The differences for these azimuths generally do not exceed 15%. The maximum reduction of modules of the reflection coefficients in comparison with these azimuths (for some angles of incidence of more than 2 times) is observed for the azimuths between 45° and 75°.

The total obtained results for all investigated azimuths and angles of incidence are shown in Fig. 5a, in form of a surface. It is also clearly seen here that at relatively small angles of incidence, the modulus of the reflection coefficient is almost independent of the azimuth. However, at large angles there is a strong azimuthal dependence of this parameter.

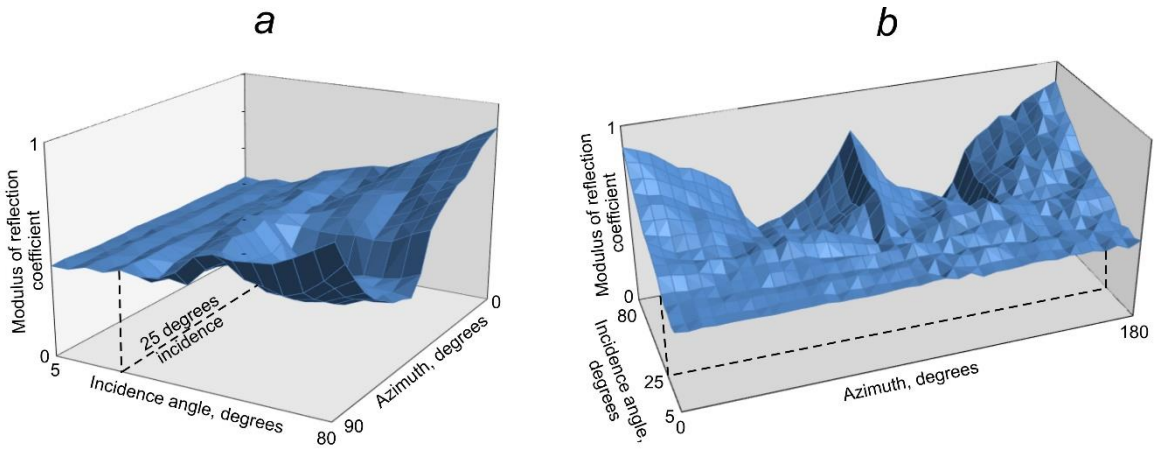

Figure 5. (a) The dependence of the reflection coefficient on the angle of incidence and azimuth of the plane of incidence relative to the direction of layering (azimuth 0° – along, 90° – across the layering); (b) the same data from a different angle, supplemented by data from the control experiment.

It is interesting to compare the obtained results with the results of experiments on the reflection of compression waves from the boundary with a high-velocity azimuthally anisotropic medium given in the article (Malehmir & Schmitt 2017). In this work, the reflection of ultrasound from the boundary of water and a high-velocity layered material (canvas fabric phenolic laminate) was investigated. As in our experiments, the reflection

coefficients were weakly dependent on the azimuth at angles of incidence less than about 25°. The authors suggested that this is a consequence of the fact that for all investigated azimuths, this range corresponds to subcritical angles. The main changes in the results of their experiments were observed just in the area of critical angles, where the reflection coefficients are maximum. Since the critical angles for the boundary with an azimuthally anisotropic high-velocity medium differ for different azimuths, the azimuthal dependence of the reflection coefficients manifests itself mainly in the change in the angles of incidence at which these maxima are observed.

In our experiments, however, when compression waves are incident on the boundary of a lower-velocity medium, critical angles are absent, since the angles of refraction into a low-velocity medium are smaller than the angles of incidence and reflection. Nevertheless, while the incidence angles are less than 25°, the reflection coefficients obtained for all azimuths are very close. However, for incidence angles greater than 25°, a significant dependence of the reflection coefficients on the azimuth is observed.

The coincidence of the "cut-off angles" (25°) in the two considered cases is, apparently, purely random. According to the results of one experiment, we cannot say whether this angle depends on the parameters of a low-velocity anisotropic medium. Although it can be assumed that such a dependence should be. At the same time, for the case of a high-velocity anisotropic medium, Malehmir & Schmitt (2017) noted the absence of an azimuthal dependence of the reflection coefficients, in particular, in the range of subcritical angles. However, for different reflective media, the critical angles can vary greatly. Therefore, the "cut-off angle" of 25° observed in the two experiments mentioned above, obviously,

cannot be considered a universal characteristic. For different materials, it can take on different values.

In addition to the main experiment, we conducted a control one, during which the azimuth of the plane of incidence varied from 90° to 180°. Since these observations should ideally give a "mirror" result in relation to the main experiment, their results allowed us to estimate the repeatability of measurements. For comparison, the data of the main and additional experiments are presented together in Fig. 5b. The quality of the data obtained in the control experiment is slightly less than the main one, since to reduce the experiment time, the measurements were carried out not with 1000-fold, but with 100-fold accumulation. Nevertheless, a comparison of the reflection coefficient modules measured at the "mirror" azimuths showed that their differences as a rule did not exceed 2–4 percent.

Although the reflection coefficients in the directions along and across the layering are close, the nature of their changes near these directions is significantly different. As the azimuth of the plane of incidence approaches the direction of the layering, the reflection coefficients change relatively smoothly. At the same time, the azimuth coinciding with the axis of symmetry, at large angles of incidence is characterized by sharp peak values of the reflection coefficient. In addition, the region with low values of reflection coefficients is shifted to the direction of the axis of symmetry.

Of course, a single experiment does not allow us to make any serious generalizations. However, if the noted features are also characteristic of other anisotropic materials, then this can be used in practice to evaluate the direction of the axis of symmetry of a low-velocity azimuthally anisotropic medium.

It is known that if compression and shear waves propagate in the isotropy plane and are polarized in the same plane, the reflection–refraction phenomena on the boundary with azimuthally anisotropic medium can be described in the same way as in the case of isotropic media with the velocities of the corresponding waves (Rüger 1997). In our experiments, this situation corresponds to an azimuth of 0° (as well as 180° in the control experiment) and velocity in an anisotropic sample V_{p1} =1110 m/s and V_{s1} =680 m/s.

We calculated the dependence of the reflection coefficient modulus on the angle of incidence for this case using a computer program for plane waves in isotropic media from paper (Young & Braile 1976). This program uses the explicit expressions for reflection coefficients given by Červený & Ravindra (1971, pp 62-64).

Note that in our experiments, the waves can be considered as practically plane (Aki & Richards 1980), since the distance from the source to the reflecting segment is greater than the wavelength at the prevailing frequency several dozen times. It can be seen from Fig. 6 that the calculated and the obtained experimental reflection coefficients are generally in good agreement. The average difference is about 2%.

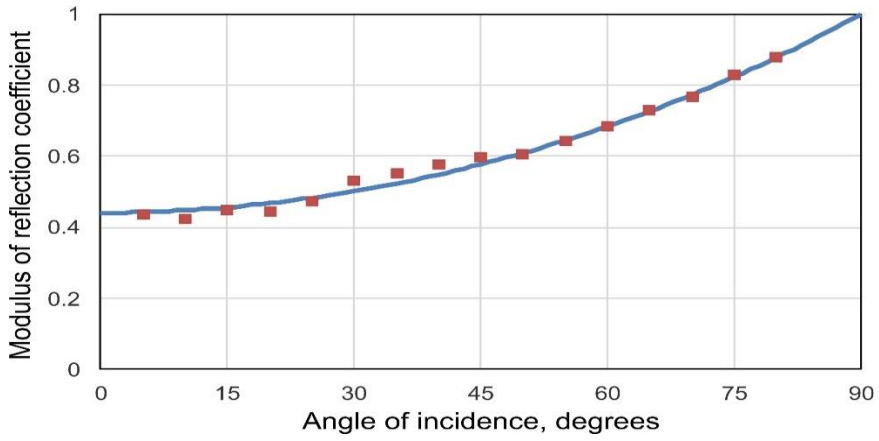

Figure 6. Comparison of experimental (square markers) and theoretical (solid line) reflection coefficients for the azimuthal direction of the plane of incidence along the layering.

Nevertheless, it must be mentioned that slightly lower (about 3.5%) values of the experimental coefficients with respect to theoretical values at angles of incidence 10°, 20° and elevated (with 5–8%) values in the range from 30° to 45° are observed both for the azimuth 0° and for the "mirror" azimuth 180°. Perhaps these regular deviations are related to the inhomogeneity of the double layers that make up the sample.

CONCLUSIONS

Our proposed the technology of layer-by-layer 3D printing with variable density of layers allows one to produce samples of materials with a high degree of anisotropy. In this paper, such sample printed on a 3D printer was used to experimentally study the reflection of ultrasound from the boundary of water with a low-velocity azimuthally anisotropic material.

The experiments have shown that the reflection of compression waves from a thin-layered low-velocity medium with a horizontal axis of symmetry can depend on the azimuth in a rather complex way. At relatively small (up to about 25°) angles of incidence the azimuthal dependence of the reflection coefficients was not observed. However, at large angles the reflection coefficient modules depending on the azimuth of the plane of incidence can both increase and decrease, and quite significantly.

At the same time, the reflection coefficient modules at the orientation of the plane of incidence along and across the layering differ slightly. This may make it difficult to determine the direction of the axis of symmetry of a low-velocity azimuthally anisotropic medium using the waves reflected from such boundary. This is the fundamental difference between the low-velocity medium and the high-velocity medium, at the boundary with which the reflection coefficients are sharply different for these two azimuths in the critical angle region. Nevertheless, the features of the dependence of the reflection coefficients on the azimuth,

namely sharp peak values at azimuths close to the direction of the axis of symmetry of the azimuthal anisotropic medium, can be used in practice to estimate the direction of this axis.

Of course, the 25° cut-off incidence angle noted above is not a universal characteristic. For azimuthally anisotropic materials with different properties, this angle may have different values. More substantiated conclusions can be drawn after further accumulation of experimental data. Nevertheless, the results obtained for the boundary with the model of a HTI medium with a very strong anisotropy allows us to predict that the dependence of the reflection coefficients on the azimuth should be manifested only at large angles of incidence. At relatively small angles of incidence, this dependence is practically not observed.

The obtained experimental results can be used to test algorithms and programs for calculating wave fields in media with azimuthally anisotropic layers, reflection coefficients for the boundaries of anisotropic media, various methods of AVO analysis, etc.

ACKNOWLEDGMENTS

This work was supported by the Russian Foundation of Basic Research (Grant # 19-05-00730) and Project AAAA-A19-119102490050-2. The authors are grateful to the employee of the Nikolaev Institute of Inorganic Chemistry SB RAS Samsonenko D.G. for assistance in the manufacture of a sample of anisotropic material.

REFERENCES

1. Aki, K. & Richards, P., 1980. *Quantitative Seismology, Theory and Methods*, 2nd edn. Vol. 1. pp 557, San Francisco: Freeman.
2. Brown, R.J., Lawton, D.C. & Cheadle S.P., 1991. Scaled physical modelling of anisotropic wave propagation: multioffset profiles over an orthorhombic medium. *Geophys. J. Int.,* **107**, 693–702.

3. Cao, Z., Li, X.-Y., Liu, J., Qin, X., Sun, S., Li, Z. & Cao, Z., 2018. Carbonate fractured gas reservoir prediction based on P-wave azimuthal anisotropy and dispersion. *J. Geophys. Eng.*, **15**, 2139–2149.
4. Červený, V. & Ravindra, R., 1971. Theory of Seismic Head Waves. pp. 312, Toronto: University of Toronto Press.
5. Chang, C.H. & Gardner, G.H.F., 1997. Effects of vertically aligned subsurface fractures on seismic reflections: A physical model study. *Geophysics*, **62**, 245–252.
6. Chang, C.H., Gardner, G.H.F. & McDonald, J.A., 1994. A physical model of shear-wave propagation in a transversely isotropic solid. *Geophysics*, **59**, 484–487.
7. Chang, C.H., Gardner, G.H.F. & McDonald, J.A., 1995. Experimental observation of surface wave propagation for a transversely isotropic medium. *Geophysics*, **60**, 185–190.
8. Chang, Y.F. & Chang, C.H., 2001. Laboratory results for the features of body-wave propagation in a transversely isotropic media. *Geophysics*, **66**, 1921–1924.
9. Cheadle, S.P., Brown, R.J. & Lawton, D.C., 1991. Orthorhombic anisotropy: A physical seismic modeling study. *Geophysics*, **56**, 1603–1613.
10. Ebrom, D., Tatham, R., Sekharan, K., McDonald, J. & Gardner, G., 1990[a]. Hyperbolic traveltime analysis of first arrivals in an azimuthally anisotropic medium: a physical modeling study. *Geophysics*, **55**, 185–191.
11. Ebrom, D.A., Tatham, R.H., Sekharan, K.K., McDonald, J.A. & Gardner, G.H.F., 1990[b]. Dispersion and anisotropy in laminated versus fractured media: An experimental comparison. *60th Annual International Meeting. Society of Exploration Geophysicists.* Expanded Abstracts. pp 1416–1419.

12. Hall, S.A. & Kendall, J.M., 2003. Fracture characterization at Valhall: Application of *P*-wave amplitude variation with offset and azimuth (AVOA) analysis to a 3D ocean-bottom data set. *Geophysics,* **68**, 1150–1160.
13. Helbig, K. & Thomsen, L., 2005. 75-plus years of anisotropy in exploration and reservoir seismics: A historical review of concepts and methods. *Geophysics*, **70**(6), 9ND–23ND.
14. Huang, L., Stewart, R., Dyaur, N. & Baez-Franceschi, J., 2016. 3D-printed rock models: Elastic properties and the effects of penny-shaped inclusions with fluid substitution. *Geophysics,* **81**, 669–677.
15. Jenner, E., 2002. Azimuthal AVO: Methodology and data examples. *The Leading Edge*, **21**, 782–786.
16. Karaev, N.A., Lukashin, Yu.P., Prokator, O.M. & Semenov, V.P., 2008. Physics modeling of a fractured media. *Seismic Technologies,* **2**, 64–73. (In Russian)
17. Kolesnikov, Yu.I., 2005. Reflection of ultrasonic pulses from the interface between water and non-perfectly elastic media: experimental data for the case of oblique incidence. *Phys. Mesomech.*, **8**, 43–48.
18. Liu, E., Chapman, M., Varela, I., Li, X., Queen J.H., & Lynn, H., 2007. Velocity and attenuation anisotropy: Implication of seismic fracture characterizations. *The Leading Edge,* **26**, 1170–1174.
19. Luan, X., Di, B., Wei, J., Zhao, J. & Li, X., 2016. Creation of synthetic samples for physical modelling of natural shale. *Geophys. Prospect*., **64**, 898–914.
20. Lynn, H.B., Simon, K.M., Bates, C.R. & Van Dok, R., 1996. Azimuthal anisotropy in *P*-wave 3-D (multiazimuth) data. *The Leading Edge,* **15**, 923–928.

21. Mah, M. & Schmitt, D.R., 2001. Experimental determination of the elastic coefficients of an orthorhombic material. *Geophysics*, **66**, 1217–1225.

22. Mahmoudian, F., Margrave, G.F., Wong, J. & Henley, D.C., 2015. Azimuthal amplitude variation with offset analysis of physical modeling data acquired over an azimuthally anisotropic medium. *Geophysics*, **80**, 21–35.

23. Malehmir, R. & Schmitt, D.R., 2017. Acoustic Reflectivity from Variously Oriented Orthorhombic Media: Analogies to Seismic Responses from a Fractured Anisotropic Crust. *J. Geophys. Res. – Sol Ea.*, **122**, 10 069–10 085.

24. Mallick, S., Craft, K.L., Meister, L.J. & Chambers, R.E., 1998. Determination of the principal directions of azimuthal anisotropy from *P*-wave seismic data. *Geophysics*, **63**, 692–706.

25. Melia, P.J. & Carlson, R.L., 1984. An experimental test of *P*-wave anisotropy in stratified media. *Geophysics*, **49**, 374–378.

26. Robertson, J., Hill, E., Plumb, A.A., Choong, S., West, S.J. & Nikitichev, D., 2016. 3D printed ultrasound phantoms for clinical training. *32nd International Conference on Digital Printing Technologies*. Volume: 32. pp. 410-415.

27. Rüger, A., 1997. *P*-wave reflection coefficients for transversely isotropic models with vertical and horizontal axis of symmetry. *Geophysics*, **62**, 713–722.

28. Tatham, R., Matthews, M., Sekharan, K., Wade, C. & Liro, L., 1992. A physical model study of shear-wave splitting and fracture intensity. *Geophysics*, **57**, 647–652.

29. Tsvankin, I., 2012. Seismic signatures and analysis of reflection data in anisotropic media, 3nd edn. pp 459: SEG.

30. Worthington, M.H., 2008. Interpreting seismic anisotropy in fractured reservoirs. *First Break.* **26**(7), 57–63.

31. Young, G.B. & Braile, L.W., 1976. A computer program for the application of Zoeppritz's amplitude equations and Knott's energy equations. *Bull. Seism. Soc Am.*, **66**, 1881–1885.

32. Zeltmann, S.E., Gupta, N., Tsoutsos, N.G., Maniatakos, M., Rajendran, J. & Karri, R., 2016. Manufacturing and Security Challenges in 3D Printing. *JOM*, **68**, 1872–1881.